

Intracranial, intratumoral implantation of drug-releasing microdevices in patients with high grade gliomas is feasible, safe, and may predict tumor response to systemic chemotherapy

Pierpaolo Peruzzi, MD, PhD (✉ pperuzzi@bwh.harvard.edu)

Brigham and Women's Hospital <https://orcid.org/0000-0001-5034-2963>

Christine Dominas

Brigham and Women's Hospital

Geoffrey Fell

Dana Farber Cancer Institute

Sarah Blitz

Harvard Medical School

Joshua Bernstock, MD, PhD

Brigham and Women's Hospital

Hassan Dawood

Brigham and Women's Hospital

Daniel Triggs, NP

Brigham and Women's Hospital

Sebastian Ahn

Brigham and Women's Hospital

Sharath Bhagavatula, MD

Brigham and Women's Hospital

Zuzana Tatarova, PhD

Brigham and Women's Hospital

Michael Pannell

Brigham and Women's Hospital

Kyla Truman

Brigham and Women's Hospital

Anna Ball

Brigham and Women's Hospital

E Antonio Chiocca, MD, PhD

Brigham and Women's Hospital

Keith Ligon, MD

Dana Farber Cancer Institute

Patrick Wen, MD

Dana Farber Cancer Institute

Oliver Jonas, PhD (✉ ojonas@bwh.harvard.edu)

Brigham and Women's Hospital

Research Article

Keywords: Gliomas, Microdevices, Drug Response, Chemotherapy, Surgery

Posted Date: May 12th, 2022

DOI: <https://doi.org/10.21203/rs.3.rs-1647435/v1>

License:   This work is licensed under a Creative Commons Attribution 4.0 International License.

[Read Full License](#)

Abstract

The lack of reliable predictive biomarkers to guide effective therapy is a major obstacle for the advancement of therapy for high grade gliomas (HGG), and particularly glioblastoma (GBM), one of the few cancers whose prognosis has not improved over the past several decades. With this pilot clinical trial we provide first in human evidence that drug-releasing intratumoral microdevices (IMD) can be safely and effectively used to obtain patient-specific, high throughput molecular and histopathological data to inform selection of drugs based on their observed antitumor effect *in situ*. The use of IMD is seamlessly integrated in standard surgical practice during tumor resection. None of the six enrolled patients experienced adverse events related to the IMD, and the retrieved tissue was usable for downstream analysis for 11 out of 12 retrieved specimens. Molecular analysis of the specimens provided, for the first time in humans, preliminary evidence of the robustness of the readout, with strong correlation between IMD analysis and clinic-radiological responses to temozolomide. From an investigational aspect, the amount of information obtained with IMD allows unprecedented characterization of tissue effects of any drugs of interest, within the physiological context of the intact tumor.

Introduction

Glioblastoma, one of the most aggressive human malignancies, was the first cancer to be dissected at the genomic level¹, pioneering the modern era of oncologic medicine. This molecular approach has led to the identification of several key driver genes (*EGFR*, *PDGFRA*, *PIK3CA*, *PTEN*, *NF1*, *RB1*, *TP53*, *IDH1*, etc) and pathways, including frequent alterations in chromatin remodeling.² While this has resulted in significant advances in diagnosis³, and prognosis⁴, it has not significantly impacted treatment^{5,6,7}. Clinical trials investigating therapies specifically targeted against major oncogenic pathways like *EGFR*⁸ or *CDK4/6*⁹ have shown no benefit. Presently, the only clinically relevant molecular biomarkers for predicting therapy response in HGG are: 1) R132H mutation in the isocitrate dehydrogenase 1 (*IDH1*) gene, which is responsible for a well-defined subfamily of tumors, and which portends a better prognosis² and possibly response to *IDH1* inhibitors¹⁰; and 2) the expression status of the O⁶ methyl-guanine methyl transferase (*MGMT*) gene, which is used as a predictor of response to DNA alkylating agents such as temozolomide (TMZ)¹¹ and lomustine¹². Use of the *MGMT* promoter methylation status for predicting therapy efficacy is fraught with limitations, such as unreliability and inconsistency of current clinical assays as well as interobserver variability¹³. Also, for the large group of patients with partial *MGMT* methylation cutoff thresholds are not well-established, leading to a grey zone in which the readout is generally inconclusive¹⁴. No clinically validated biomarkers exist for the prediction of tumor sensitivity for the range of other therapies in HGG.

The disconnect between the abundance of molecular data available from each tumor and its lack of practical therapeutic value is due to many factors. Firstly, *in vitro* and *in vivo* models, which are used to test drug effects, are often suboptimal and yield results which are not recapitulated in patients¹⁵. Secondly, the notorious heterogeneity of GBM cell populations^{16,17} makes it difficult to generalize

biological responses across all the different cellular subtypes of the tumor, let alone among different patients. Thirdly, redundant oncogenic pathways^{2,18} and pronounced epigenetic plasticity characteristic of glioma cells¹⁹ make these tumors exquisitely adaptable and insensitive to isolated molecular hits.

For these reasons, Lab-in-a-Patient approaches have been gaining traction in recent years as a potentially more effective way to establish the benefit of experimental treatments, in a personalized manner. Modern phase 0, window of opportunity clinical studies, where experimental drugs are given systemically before tumor resection, have demonstrated their value in providing important information, including tissue concentrations, cell responses and molecular biomarkers^{20,21,22}. However, they still suffer from profound limitations, in particular the fact that each patient is exposed to only one drug at a time, making this design unsuitable for high throughput efficacy screening. Additionally, they cannot provide a comparison of effectiveness among different drugs, cannot test the effect of drug combinations and, finally, remain significantly resource-intensive.

To fill this gap, and facilitate a high throughput approach towards a personalized drug screening on a patient-by-patient basis, we developed a novel intrasurgical approach that takes advantage of the operational window provided by standard of care craniotomies for tumor resection to probe a patient's glioma with different pharmacological perturbations directly within its native microenvironment (Fig. 1), in order to obtain critical data on the personalized comparative drug responses which to-date have been elusive to the field.

Our approach is based on tiny (6 x 0.7 mm) bio-compatible intratumoral microdevices (IMD)²³ (Fig. 1a) which are inserted into the tumor at the time of surgery and remain in place until the tumor is fully resected. During this time, they release nanodoses of drugs in a spatially confined manner, such that they do not overlap (Fig. 1b,c). Nanodoses are defined as amounts of drugs which result in negligible systemic concentrations (in our approach ~ 1/100,000th of what is achieved during normal dosing) but are able to provide appropriate concentrations in the tissue immediately adjacent (~ 0.5-1mm) to the point of release²⁴. After incubation, the exposed tissue is collected, and the effect of each drug on the tumor is assessed independently and in parallel, allowing multiplexed pharmacological measurements (Fig. 1c,d).

Here we report the results of a first-in-human pilot clinical trial in high grade glioma patients, which provides evidence of safety, efficient integration into the standard clinical workflow, and technical feasibility. Robust drug phenotypes are obtained for a wide range of anti-cancer agents within the time of incubation afforded by standard surgical resection, and thus allowing full integration and virtually no interference with standard surgical and clinical practice. Importantly, we find early evidence that IMD readouts of intratumor microdose drug effect directly correlate with tumor response to systemic chemotherapy in GBM patients. Our findings support the use of this platform as a novel approach to identifying treatment options for brain tumor patients, integrating the data obtained from IMD in the decisional algorithm of a most effective, fully personalized adjuvant pharmacologic therapy.

Methods

Trial design

This is an investigator-initiated, non randomized, single-center phase 1 study. All patients underwent surgery and follow up at the Brigham and Women's Hospital and Dana Farber Cancer Institute, both affiliated to Harvard Medical School, Boston, USA. After obtaining IND approval for use of IMDs, all aspects of the trial were approved on 10/23/2019 by the Institutional Review Board (IRB) at the Dana Farber Cancer Institute under protocol number 18–623. The study was registered at <https://clinicaltrials.gov> under the identifier NCT04135807. The purpose of this study was explorative, to investigate safety and feasibility of integrating IMD use during an otherwise standard brain surgery for tumor resection. Consequently, as specified in the trial consent, no information obtained from the IMD was used to make medical decisions regarding the post-surgical care of patients.

Patient Selection and Enrollment

The trial was open to any patients older than 18 years of age, with known or suspected supratentorial glioma (WHO grade 2–4) observed in a brain MRI with and without intravenous gadolinium, and for which a craniotomy for tumor resection was indicated. The required lesion volume was greater than 5 cubic centimeters. A Karnofsky Performance Score (KPS) ≥ 60 was also required. Exclusion criteria were enrollment in concomitant trials. Patients with coagulopathies, platelet counts $< 100,000/\text{ml}$, or with deep-seated tumors (in brainstem and/or thalamus) were also excluded. Eligibility was assessed in clinic and details were explained before an informed consent was obtained.

The accrual diagram is presented in Supplementary Fig. 1.

IMD development

IMDs were manufactured from implant-grade radiopaque poly-ether-ketone-ketone (PEKK) with 20% barium sulfate (Oxford Performance Materials) on a 5-axis CNC micromachining station using subtractive machining techniques and inspected in accordance to quality control guidelines, as previously described²⁵. A rigid nitinol guidewire of 0.25 mm diameter, designed to increase visualization of the devices in the operatory field and within the specimen, was attached to the IMD body using medical-grade epoxy (EPO-TEK MED-301) and a curing step. IMDs were rinsed in United States Pharmacopeia (USP)-grade Sodium Hydroxide and endotoxin-free water²⁶.

All pharmaceutical agents used are FDA-approved and purchased commercially. The list of drugs and their mechanism of action is provided in Fig. 1b. The drugs were prepared, mixed with USP-grade PEG matrix, and loaded. IMDs were singularly placed into 15 ml polypropylene tubes and into a sterilization pouch. Pouches were sent for gamma irradiation, followed by endotoxin and sterility testing, before they were stored in the operating room pharmacy for off-the-shelf use.

Intraoperative IMD insertion

For every patient, surgery proceeded as per standard neurosurgical practice. All surgeries were performed by the first author (PP), for the benefit of procedural consistency. After exposure of the brain surface and

localization of the lesion, either by direct visualization or through image-guided means (neuronavigation or ultrasound), an intraoperative biopsy was obtained (Extended data Fig. 1a), as confirmation of the nature of the lesion via frozen histopathology analysis was required before proceeding with IMD implantation. Up to two IMDs per patient were implanted, by holding the IMD with fine tweezers, in a peripheric region of the tumor, so that resection of the rest of the tumor could proceed while the IMD remained indwelled within the tissue (Extended data Fig. 1b). The IMD were inserted into tissue for their entire length, so that their terminal bevel was anchored just underneath the pia mater, increasing their stability. The nitinol tail remained visible during the entire time (Extended data Fig. 1c-f), to minimize unvoluntary displacement of the IMD and to facilitate its retrieval.

IMD retrieval

At the end of resection, the small part of tumor containing the IMD was removed under operating microscope visualization, assuring that at least 1 cm of untouched tissue around the IMD was recovered. Immediately upon removal, the specimen was placed in liquid nitrogen or dry ice and transported to the lab for downstream analysis (Extended data Fig. 1e, f).

Specimen analysis

For every patient, a fragment of tumor was sent to the pathology laboratory for standard diagnostic immunohistochemistry, *MGMT* promoter methylation analysis, and genetic profiling by next generation sequencing analysis. The remainder of the tissue was used for additional exploratory correlative studies.

The tumor specimen containing the IMD was snap-frozen immediately upon surgical resection. The tumor-device specimen was sectioned on a standard cryotome, and several serial tissue sections of 8µm thickness were collected at each drug reservoir level of the IMD, as previously described²⁷. Imaging of drug autofluorescence and quantitation was performed as previously described²⁸.

These sections then underwent immunofluorescence (IF) staining for antibodies against pH2AX, cleaved caspase 3 (CC3) and other markers (Cell Signaling) on a Leica Bond Autostainer. A detailed description of the quantitative pipeline used for automated scoring of IF marker expression was previously described²⁸. In brief, a concentric segment of the tumor/device cross-section corresponding to the region of drug distribution is selected for each drug reservoir, with dimensions of 400 x 800µm. Within this region of interest, the total number of cells which stain positive for a given marker (e.g. pH2AX) are counted using automated counting by CellProfiler, and the value is divided by the total number of cells in this region as determined by Dapi staining.

Statistical analysis

This study had two co-primary endpoints, safety and feasibility. Both were powered using a beta-binomial distribution. For safety, we assumed a dose limiting toxicity (DLT) rate = 5%. For feasibility we assumed a device failure rate = 5%.

IMD safety was measured at the patient level and monitored through incidence of adverse events. The limiting toxicities were defined as either a grade 3 or higher adverse event associated with the IMD, or situations where the IMD becomes lost or unretrievable. The device would be considered unsafe if ≥ 3 limiting toxicities were observed in the first 6 patients, or ≥ 4 in a total of 12 patients.

IMD futility was measured at the device level, defined as the successful extraction of the implanted device containing viable tissue for histopathologic analysis. We considered the procedure successful if the estimate for retrievable success rate had a lower bound that exceeded 50%.

The summary statistic for safety and futility were estimated as 90% binomial confidence intervals (CI). Continuous measures were reported as means with standard deviation, while categorical measures as counts and percentages.

All laboratory experiments and data analysis were performed at least in triplicates (except for patient 4, the only instance where only one IMD could be used), reporting both mean and standard deviation for each data set. The data points were plotted and analyzed using GraphPad Prism version 9.0.

Results

Patient Characteristics

A total of 6 patients were enrolled in this study between April 2020 and August 2021. There was an equal frequency of female and male individuals (50% each). Median age was 76 years old, with a range between 27 and 86. Five patients were diagnosed with glioblastoma, while the remaining patient had grade 4 astrocytoma (due to the presence of *IDH1* mutation), according to the most recent WHO classification³. Five out of 6 (83%) were newly diagnosed tumors, and naïve to prior chemoradiation, while the remaining patient had tumor recurrence after radiation and temozolomide, followed by lomustine at the time of the first recurrence, and before trial enrollment. Tumor size averaged 81 cc (measured by the ellipsoid formula $\frac{1}{2} \times \text{Length} \times \text{Width} \times \text{Depth}$), with a range between 26.8 and 129 cc. Five out of 6 tumors (83%) had wild type *IDH1* gene, while one had the R132H mutation. Three tumors (50%) were partially methylated in the *MGMT* promoter, two (33%) were non-methylated and one (16%) was methylated. Four out of 6 patients (66%) underwent craniotomy under general anesthesia, while two (34%) were operated under conscious sedation (i.e. “awake surgery”) due to tumor involvement of eloquent regions (Extended data Table 1).

Primary endpoint 1: Safety

Postoperative follow up for each patient was performed daily for the first 3 days after surgery, then at 12 ± 2 days and finally at 30 ± 4 days. There were no immediate (< 48 hours after surgery), nor delayed (< 30 days) adverse events (AEs). Twelve out of 12 inserted IMD (100%; 90% CI (61%-100%)) were successfully retrieved and none was lost or abandoned in the patient. All postoperative bloodwork, obtained on postoperative days 1 and 2, remained stable compared to preoperative values. Postoperative brain MRI

with and without IV gadolinium was obtained within 48 hours after surgery: Gross Total Resection (GTR), i.e. the removal of all contrast enhancing tissue was achieved in 5 out of 6 (83%) patients, while Subtotal Resection (STR) (residual contrast enhancing nodule $\leq 5 \text{ cc}^{29}$) was obtained in the remaining patient (Extended data Table 1).

Primary Endpoint 2: Feasibility and integration with neurosurgical practice

Eleven out of 12 (92%; 90% CI (66%-100%)) total implanted IMD provided specimens which could be successfully processed for the downstream molecular analysis. The only exception was due to inadvertent microdevice dislodgement of one IMD during tumor resection in patient 4. Each specimen was successfully aliquoted into multiple samples which allowed different molecular analysis protocols (i.e. multiplexed immuno-histochemistry, transcriptional analysis, and Mass spectrometry analysis) to be carried out simultaneously from the same tissue. Microdevices remained indwelled *in situ* into living tumor tissue for an average of 136 minutes during tumor resection (range 122–155 minutes, SD 11 minutes). The time between specimen removal and freezing was < 1 minute in all cases (Table 1).

The use of microdevices had a very low footprint on the surgery performance and in all other aspects of clinical care: In comparison to a control cohort of nine patients with gliomas who underwent surgery by the same operator (PP) during the same timeframe of this trial, but who were not included in the trial (due to participation in other trials, inability to consent, or not meeting inclusion criteria), the application of IMD did not result in significant changes in the surgical procedure and its aftermath: length of surgery (skin incision to skin closure) was slightly increased in the trial patients (300 minutes Vs 230 minutes), due to the need to wait for intraoperative biopsy results before proceeding with IMD implantation. However the differences were not statistically significant. Length of postoperative Intensive Care Unit (ICU) stay or total hospital stay were not different (Extended data Fig. 2). Also, surgical costs did not increase in patients receiving the microdevices. Only a 15% increase in Pathology Lab costs (\$14,000-MD vs \$12,000-standard surgery) was detected in trial patients, but the difference was not significant.

Measurement of localized intratumor drug release

Each of the pharmaceutical agents loaded into the IMD reservoirs is released upon implantation into a confined region of the tumor directly adjacent to its reservoir. The local concentration is determined by the ratio of drug versus PEG polymer in the formulation, and the release kinetics and diffusion distance are controlled by the molecular weight of the polymer being used. We demonstrate uniformity of release and tissue transport for two agents with opposite solubility properties: doxorubicin which is water-soluble, and lapatinib which is insoluble. These drugs were chosen because they are readily detected and quantitated by autofluorescence. Figure 2a,c describes the release profile for each agent. We observe a distance-dependent concentration gradient where higher concentrations are present at the device-tissue interface, and decrease gradually with increasing radial distance from the reservoir. The presence of drug in the tissue at the correct reservoir site also confirms that the IMD did not move during the implantation time in the tumor or during excision and processing. Figure 2b,d describe the maximum and average intratumor

drug concentrations over the region of drug release. We observe only moderate variability in the diffusion curves of < 20% from the mean in the maximum exposure concentrations, and < 15% in the average drug exposure, across all six patients.

Measurement of tumor drug sensitivity and identification of response biomarkers

In each patient sample, we determined the tumor sensitivity to drugs by measuring the expression of cleaved-caspase-3 (CC3), a marker for apoptosis, and p-H2AX, a marker for DNA damage, in each drug exposed tumor section. Our first analysis focused on the tumor sensitivity to temozolomide (TMZ), as this is the most widely used agent in this patient population and offered the opportunity to compare the IMD readout with clinic-radiological response to the drug. TMZ is a DNA alkylating agent which causes apoptosis by inducing DNA damage³⁰. Thus, DNA damage, measured by p-H2AX, is an early marker of drug effect for agents such as TMZ³¹. Figure 3a shows the level of p-H2AX and cleaved caspase 3 (CC3) induced by TMZ in each patient tumor across multiple spatially distant tumor regions from different microdevice reservoirs implanted in the same patient.

The highest level of DNA damage was observed in Patient 3 (65.8% of cells in drug exposed region), and the lowest levels in Patients 5 and 6 (9.8% and 17.7%, respectively), with the corresponding differences between Patient 3 versus Patients 5 and 6 being highly statistically significant.

Representative IHC images which show the spatial relationship between IMD, the tumor tissue, and biomarkers are presented in Extended data Fig. 3.

Apoptosis induction as measured by CC3 expression was generally low (< 5%), except in Patient 3 where it was expressed in 13.1% of cells. This represents a statistically significant difference between CC3 response to TMZ in Patient 3 versus Patients 5 and 6 (Fig. 3a). Since the time of drug exposure was relatively short, CC3, a marker of apoptosis, was not expected to be highly expressed yet in the samples³².

Determination of concentration dependence of anti-tumor effect for temozolomide:

We exploited the distance-dependent concentration gradient of drugs eluting from the IMD (shown in Fig. 2) to determine the dose dependence of the anti-tumor effect for TMZ (Fig. 3b). We generally observe high DNA damage scores at the immediate vicinity to the drug reservoir which corresponds to the highest concentration, and sharply declining sensitivity at lower doses. Patient 3 exhibits the highest IMD response across the entire concentration range, and maintains > 40% of cells with confirmed pH2AX down to 0.1 μ M. Patient 5 shows the lowest response across all TMZ concentrations (< 10%).

Intratumor TMZ dose from systemic administration was not measured, and there is still generally a lack of available data on intratumor drug levels for most agents. As more such data are obtained, the measurements of dose-dependent effect provided by the IMD may provide insight into minimum required

intratumor concentrations to obtain threshold levels of DNA damage or apoptosis that need to be reached for durable effects, which may in turn inform systemic dosing regimens. Such thresholds for localized drug efficacy will be defined in subsequent larger studies.

Correlation between microdose intratumor drug responses, and clinical responses to systemic treatment

Temozolomide (TMZ) is the most widely used drug in GBM, and the only drug with which some patients in our trial were treated systemically, as part of the standard of care. Thus, although our trial was not designed to choose chemotherapy agents based on IMD data, we still could compare the observed clinical/radiological response to systemic TMZ with the patient-specific response to TMZ in the IMD-exposed tissue. Patient 1, 2 (partial *MGMT* methylation) and 4,6 (no *MGMT* methylation) all showed none to minimal response to TMZ in the IMD, as measured by p-H2AX expression in the drug-treated region. Of these, only patient 6 received adjuvant TMZ, with no observed benefit, in keeping with the poor tissue response observed in the IMD analysis (Fig. 3a). None of the other three patients received adjuvant TMZ, and therefore no direct connection could be established between IMD readout and clinical response.

On the contrary, patient 3, a 72 year old female with partially methylated *MGMT* promoter, *IDH1*-wt GBM and whose IMD analysis predicted significant response to TMZ, had an overall survival of more than 18 months after receiving systemic TMZ (Fig. 4), and despite being the only patient of the cohort not to have gross total resection, in itself a poor prognostic factor³³. At the present time, this patient remains alive and clinically stable. In this specific case, the patient's *MGMT* promoter methylation status, assessed with the gold standard bisulfite sequencing analysis³⁴, would not have predicted the significant clinical response that was observed, while the IMD correctly predicted the response. Conversely, patient 6, an 81 year old female with NON-methylated *MGMT* promoter, *IDH1*-wt GBM and whose IMD analysis predicted no response to TMZ, experienced clinical and radiological evidence of tumor progression 6 months after treatment and proceeded to palliative Avastin. This, despite gross total tumor resection and receiving the same adjuvant treatment as patient 3.

Patient 5, a 27 year old male with recurrent GBM, methylated *MGMT* promoter and mutated *IDH1* underwent surgery after previous failure of TMZ and confirmed radiological progression while on lomustine. In this patient, IMD analysis showed no effect to those two drugs, confirming the lack of efficacy which was already observed clinically and radiologically, despite the favorable *MGMT* promoter status (Fig. 4).

Measurement of drug sensitivity for other agents to generate treatment hypotheses

We investigated the sensitivity of each tumor to other commonly used agents in GBM which were present in the IMD but were not administered systemically to any patients in the trial. For each drug, the relative sensitivity of each patient is shown in Fig. 5. Interestingly, we observed that Patient 5 (the only recurrent

tumor) was generally resistant to all tested drugs, possibly confirming the mounting evidence that recurrent GBM is generally less responsive to any interventions³⁵. Also, patient 6 (non-methylated tumor) appeared to be potentially sensitive to several other drugs, a finding which, if confirmed, could support the strategy to use alternative drugs as a first line treatment for these particularly difficult to treat patients.

Discussion

Obtaining phenotypic information on tumor responses to drugs to enable precision medicine remains an unmet need in the treatment of gliomas. With this first-in-human pilot trial, we provide evidence of safety and feasibility for the use of intratumoral, drug-releasing microdevices as a novel approach to characterize and compare the efficacy of different pharmacologic therapies in patients with gliomas, in a personalized manner.

The main goals of this study were to demonstrate that microdevices can be easily incorporated into standard neurosurgical practice, with minimal impact to the operative protocols, no significant burden on healthcare costs, and no evidence of adverse effects, while providing valuable biological data which can be integrated with, and potentially be superior to other currently used biomarkers. The amount of information obtained with this approach, which directly integrates surgery with bioengineering, pharmacology and cancer genetics, provides a solid argument for a revisitation of surgical practice for glioma patients, where such *in-situ* investigational devices could become the norm in the future.

One potentially limiting aspect of this study is the relatively short indwelling time of the microdevices which was dictated by the need to minimize changes to the current standard of patient care (hereby the decision to not submit patients to an additional invasive IMD implantation procedure several days before surgery). During the available ~ 2.3h incubation period, we demonstrate the detection of early markers of drug effects by inducing cellular stress response in a drug and concentration dependent manner. We observe robust activation of early markers of DNA damage (phosphorylation of Histone Gamma), and low to moderate activation of molecular cascades which lead to cell death (cleaved caspase 3). Importantly, we find that the level of pH2AX expression in response to temozolomide treatment is congruent with molecular characterization of the patient's tumor, and directly predicts the clinical responses observed across each of the patients which received systemic TMZ treatment. This is particularly striking in the case of patients 3 and 5, where *MGMT* promoter methylation status by itself was not predictive of clinical response, which was correctly identified by the IMD measurement.

Larger clinical studies will be needed to confirm the predictive capability of the IMD to identify systemic responders, and to quantitatively define exact thresholds of IMD response correlating with favorable clinical outcome. We have focused the current study on agents that are routinely used in GBM. For agents that do not penetrate the Blood Brain Barrier, IMD readouts of intratumor effect may help determine minimum effective intratumor concentrations required, and this could guide the decision to implement different delivery techniques, such as convection-enhanced or nanoparticle mediated delivery, to achieve sufficient intratumor drug levels.

While the current study focused on rapidly acting cytotoxic and targeted agents, the length of exposure is likely not enough to detect changes in adaptive immune response, which have been shown to occur over the course of two days or longer³⁶.

Supported by the evidence of safety and non-futility provided with this first study iteration, a follow up clinical trial evaluating safety and feasibility of a two-staged procedure (insertion by a minimally invasive procedure, and retrieval 72 hours later by craniotomy) is currently underway. This will provide data to compare biological readouts between short and long exposures, and define whether a two-surgery approach is necessary to maximize data, or if the predictive values obtained with a single surgery and shorter exposure is sufficient to reliably inform therapy.

In addition to providing the ability to directly test a range of drugs in a patient, the use of IMDs in gliomas offer significant opportunities to answer questions which so far have been elusive: Firstly, this strategy allows to safely test the efficacy of drug combinations, which are commonly used in other cancers³⁷, but only rarely in glioblastomas, despite significant preclinical evidence that different drugs acting synergistically against redundant oncogenes are more potent than single drugs^{38,39}.

Secondly, the analysis of microdevice-exposed specimens allows a realistic vantage point into the tumor microenvironment, and particularly how drugs also affect non neoplastic cells (like immune cells, astrocytes and neurons). For example, it is still not clear how drugs modulate the anti-tumor immune response: chemotherapy is generally believed to be immunosuppressive⁴⁰. However, while some have confirmed a detrimental effect of TMZ against T and B cells in mouse models of GBM, with resultant further impairment of an already weak antitumor response⁴¹, others have shown that TMZ might preferentially deplete immune-suppressive CD4 regulatory T cells (Tregs)^{42,43}. In theory, any drugs might display unexpected effects against non-tumor cells, which, in turn, can impact clinical outcomes.

IMDs also can address the unanswered question of how glioma cell heterogeneity influences response to each drug, characterizing how different tumor subtypes respond differently to the same drug, and how tumor heterogeneity can lead to recurrence.

Finally, by providing a measurable drug gradient within the specimen, which is easily achievable through detection by autofluorescence (Fig. 2), or using MALDI mass spectrometry⁴⁴, the analysis of microdevice specimens allows quantification of tissue concentrations at which each drug is biologically effective against the tumor.

In conclusion, the direct use of IMDs in patients with gliomas represents a novel, feasible and promising approach that addresses the need to maximize efficacy of multiple pharmacotherapies, as well to understand their mechanisms of action in the most representative and predictive model.

Declarations

Clinical Trial Registry Number: NCT04135807

Contributions

Study design: PP, PYW, OJ, EAC; Molecular/laboratory studies: CD, SA, SKB, ZT, OJ; Surgeries: PP; Clinical data and trial regulatory management: PP, SB, JB, DVT, KT, MP, AB, HYD. Neuropathology : KLL. Statistical Analysis: GF.

PP wrote the manuscript with inputs and feedback from all other authors.

Competing Interests

OJ is a consultant to Kibur Medical. Dr. Jonas's interests were reviewed and are managed by BWH and Mass General Brigham in accordance with their conflict of interest policies.

All other authors do not have COI related to this manuscript.

Data availability

Any data which are not immediately available in the manuscript are available on request from the corresponding author (PP.) Those data are not publicly available due to patient privacy.

References

1. Cancer Genome Atlas Research Network. Comprehensive genomic characterization defines human glioblastoma genes and core pathways. *Nature*. 2008 Oct 23;455(7216):1061-8. doi: 10.1038/nature07385
2. Bhaskaran V, Nowicki MO, Idriss M, Jimenez MA, Lugli G, Hayes JL, Mahmoud AB, Zane RE, Passaro C, Ligon KL, Haas-Kogan D, Bronisz A, Godlewski J, Lawler SE, Chiocca EA, Peruzzi P. The functional synergism of microRNA clustering provides therapeutically relevant epigenetic interference in glioblastoma. *Nat Commun*. 2019 Jan 25;10(1):442. doi: 10.1038/s41467-019-08390-z.
3. Louis DN, Perry A, Wesseling P, Brat DJ, Cree IA, Figarella-Branger D, Hawkins C, Ng HK, Pfister SM, Reifenberger G, Soffietti R, von Deimling A, Ellison DW. The 2021 WHO Classification of Tumors of the Central Nervous System: a summary. *Neuro Oncol*. 2021 Aug 2;23(8):1231–1251. doi: 10.1093/neuonc/noab106.
4. Katsigiannis S, Grau S, Krischek B, Er K, Pintea B, Goldbrunner R, Stavrinou P. MGMT-Positive vs MGMT-Negative Patients With Glioblastoma: Identification of Prognostic Factors and Resection Threshold. *Neurosurgery*. 2021 Mar 15;88(4):E323-E329. doi: 10.1093/neuros/nyaa562.
5. Stupp R, Mason WP, van den Bent MJ, Weller M, Fisher B, Taphoorn MJ, Belanger K, Brandes AA, Marosi C, Bogdahn U, Curschmann J, Janzer RC, Ludwin SK, Gorlia T, Allgeier A, Lacombe D, Cairncross JG, Eisenhauer E, Mirimanoff RO; European Organisation for Research and Treatment of Cancer Brain Tumor and Radiotherapy Groups; National Cancer Institute of Canada Clinical Trials

- Group. Radiotherapy plus concomitant and adjuvant temozolomide for glioblastoma. *N Engl J Med*. 2005 Mar 10;352(10):987 – 96. doi: 10.1056/NEJMoa043330.
6. Lim-Fat MJ, Youssef GC, Touat M, Iorgulescu JB, Whorral S, Allen M, Rahman R, Chukwueke U, McFaline-Figueroa JR, Nayak L, Lee EQ, Batchelor TT, Arnaout O, Peruzzi PP, Chiocca EA, Reardon DA, Meredith D, Santagata S, Beroukhim R, Bi WL, Ligon KL, Wen PY. Clinical utility of targeted next generation sequencing assay in IDH-wildtype glioblastoma for therapy decision-making. *Neuro Oncol*. 2021 Dec 8: noab282. doi: 10.1093/neuonc/noab282.
 7. Wen PY, Weller M, Lee EQ, Alexander BM, Barnholtz-Sloan JS, Barthel FP, Batchelor TT, Bindra RS, Chang SM, Chiocca EA, Cloughesy TF, DeGroot JF, Galanis E, Gilbert MR, Hegi ME, Horbinski C, Huang RY, Lassman AB, Le Rhun E, Lim M, Mehta MP, Mellinghoff IK, Minniti G, Nathanson D, Platten M, Preusser M, Roth P, Sanson M, Schiff D, Short SC, Taphoorn MJB, Tonn JC, Tsang J, Verhaak RGW, von Deimling A, Wick W, Zadeh G, Reardon DA, Aldape KD, van den Bent MJ. Glioblastoma in adults: a Society for Neuro-Oncology (SNO) and European Society of Neuro-Oncology (EANO) consensus review on current management and future directions. *Neuro Oncol*. 2020 Aug 17;22(8):1073–1113. doi: 10.1093/neuonc/noaa106.
 8. Weller M, Butowski N, Tran DD, Recht LD, Lim M, Hirte H, Ashby L, Mechtler L, Goldlust SA, Iwamoto F, Drappatz J, O'Rourke DM, Wong M, Hamilton MG, Finocchiaro G, Perry J, Wick W, Green J, He Y, Turner CD, Yellin MJ, Keler T, Davis TA, Stupp R, Sampson JH; ACT IV trial investigators. Rindopepimut with temozolomide for patients with newly diagnosed, EGFRvIII-expressing glioblastoma (ACT IV): a randomised, double-blind, international phase 3 trial. *Lancet Oncol*. 2017 Oct;18(10):1373–1385. doi: 10.1016/S1470-2045(17)30517-X.
 9. Miller TW, Traphagen NA, Li J, Lewis LD, Lopes B, Asthagiri A, Loomba J, De Jong J, Schiff D, Patel SH, Purow BW, Fadul CE. Tumor pharmacokinetics and pharmacodynamics of the CDK4/6 inhibitor ribociclib in patients with recurrent glioblastoma. *J Neurooncol*. 2019 Sep;144(3):563–572. doi: 10.1007/s11060-019-03258-0.
 10. Mellinghoff IK, Ellingson BM, Touat M, Maher E, De La Fuente MI, Holdhoff M, Cote GM, Burris H, Janku F, Young RJ, Huang R, Jiang L, Choe S, Fan B, Yen K, Lu M, Bowden C, Steelman L, Pandya SS, Cloughesy TF, Wen PY. Ivosidenib in Isocitrate Dehydrogenase 1-Mutated Advanced Glioma. *J Clin Oncol*. 2020 Oct 10;38(29):3398–3406. doi: 10.1200/JCO.19.03327.
 11. Brandner S, McAleenan A, Kelly C, Spiga F, Cheng HY, Dawson S, Schmidt L, Faulkner CL, Wragg C, Jefferies S, Higgins JPT, Kurian KM. MGMT promoter methylation testing to predict overall survival in people with glioblastoma treated with temozolomide: a comprehensive meta-analysis based on a Cochrane Systematic Review. *Neuro Oncol*. 2021 Sep 1;23(9):1457–1469. doi: 10.1093/neuonc/noab105.
 12. Herrlinger U, Tzaridis T, Mack F, Steinbach JP, Schlegel U, Sabel M, Hau P, Kortmann RD, Krex D, Grauer O, Goldbrunner R, Schnell O, Bähr O, Uhl M, Seidel C, Tabatabai G, Kowalski T, Ringel F, Schmidt-Graf F, Suchorska B, Brehmer S, Weyerbrock A, Renovanz M, Bullinger L, Galldiks N, Vajkoczy P, Misch M, Vatter H, Stuplich M, Schäfer N, Kebir S, Weller J, Schaub C, Stummer W, Tonn JC, Simon M, Keil VC, Nelles M, Urbach H, Coenen M, Wick W, Weller M, Fimmers R, Schmid M,

- Hattingen E, Pietsch T, Coch C, Glas M; Neurooncology Working Group of the German Cancer Society. Lomustine-temozolomide combination therapy versus standard temozolomide therapy in patients with newly diagnosed glioblastoma with methylated MGMT promoter (CeTeG/NOA-09): a randomised, open-label, phase 3 trial. *Lancet*. 2019 Feb 16;393(10172):678–688. doi: 10.1016/S0140-6736(18)31791-4.
13. Mansouri A, Hachem LD, Mansouri S, Nassiri F, Laperriere NJ, Xia D, Lindeman NI, Wen PY, Chakravarti A, Mehta MP, Hegi ME, Stupp R, Aldape KD, Zadeh G. MGMT promoter methylation status testing to guide therapy for glioblastoma: refining the approach based on emerging evidence and current challenges. *Neuro Oncol*. 2019 Feb 14;21(2):167–178. doi: 10.1093/neuonc/noy132.
 14. Ben-David U, Siranosian B, Ha G, Tang H, Oren Y, Hinohara K, Strathdee CA, Dempster J, Lyons NJ, Burns R, Nag A, Kugener G, Cimini B, Tsvetkov P, Maruvka YE, O'Rourke R, Garrity A, Tubelli AA, Bandopadhyay P, Tsherniak A, Vazquez F, Wong B, Birger C, Ghandi M, Thorner AR, Bittker JA, Meyerson M, Getz G, Beroukhim R, Golub TR. Genetic and transcriptional evolution alters cancer cell line drug response. *Nature*. 2018 Aug;560(7718):325–330. doi: 10.1038/s41586-018-0409-3.
 15. Ben-David U, Ha G, Tseng YY, Greenwald NF, Oh C, Shih J, McFarland JM, Wong B, Boehm JS, Beroukhim R, Golub TR. Patient-derived xenografts undergo mouse-specific tumor evolution. *Nat Genet*. 2017 Nov;49(11):1567–1575. doi: 10.1038/ng.3967.
 16. Verhaak RG, Hoadley KA, Purdom E, Wang V, Qi Y, Wilkerson MD, Miller CR, Ding L, Golub T, Mesirov JP, Alexe G, Lawrence M, O'Kelly M, Tamayo P, Weir BA, Gabriel S, Winckler W, Gupta S, Jakkula L, Feiler HS, Hodgson JG, James CD, Sarkaria JN, Brennan C, Kahn A, Spellman PT, Wilson RK, Speed TP, Gray JW, Meyerson M, Getz G, Perou CM, Hayes DN; Cancer Genome Atlas Research Network. Integrated genomic analysis identifies clinically relevant subtypes of glioblastoma characterized by abnormalities in PDGFRA, IDH1, EGFR, and NF1. *Cancer Cell*. 2010 Jan 19;17(1):98–110. doi: 10.1016/j.ccr.2009.12.020.
 17. Gularyan SK, Gulin AA, Anufrieva KS, Shender VO, Shakhparonov MI, Bastola S, Antipova NV, Kovalenko TF, Rubtsov YP, Latyshev YA, Potapov AA, Pavlyukov MS. Investigation of Inter- and Intratumoral Heterogeneity of Glioblastoma Using TOF-SIMS. *Mol Cell Proteomics*. 2020 Jun;19(6):960–970. doi: 10.1074/mcp.RA120.001986.
 18. Liu Y, Li Z, Zhang M, Zhou H, Wu X, Zhong J, Xiao F, Huang N, Yang X, Zeng R, Yang L, Xia Z, Zhang N. Rolling-translated EGFR variants sustain EGFR signaling and promote glioblastoma tumorigenicity. *Neuro Oncol*. 2021 May 5;23(5):743–756. doi: 10.1093/neuonc/noaa279.
 19. Neftel C, Laffy J, Filbin MG, Hara T, Shore ME, Rahme GJ, Richman AR, Silverbush D, Shaw ML, Hebert CM, Dewitt J, Gritsch S, Perez EM, Gonzalez Castro LN, Lan X, Druck N, Rodman C, Dionne D, Kaplan A, Bertalan MS, Small J, Pelton K, Becker S, Bonal D, Nguyen QD, Servis RL, Fung JM, Mylvaganam R, Mayr L, Gojo J, Haberler C, Geyeregger R, Czech T, Slavc I, Nahed BV, Curry WT, Carter BS, Wakimoto H, Brastianos PK, Batchelor TT, Stemmer-Rachamimov A, Martinez-Lage M, Frosch MP, Stamenkovic I, Riggi N, Rheinbay E, Monje M, Rozenblatt-Rosen O, Cahill DP, Patel AP, Hunter T, Verma IM, Ligon KL, Louis DN, Regev A, Bernstein BE, Tirosh I, Suvà ML. An Integrative Model of Cellular

- States, Plasticity, and Genetics for Glioblastoma. *Cell*. 2019 Aug 8;178(4):835–849.e21. doi: 10.1016/j.cell.2019.06.024.
20. Vigneswaran K, Boyd NH, Oh SY, Lallani S, Boucher A, Neill SG, Olson JJ, Read RD. YAP/TAZ Transcriptional Coactivators Create Therapeutic Vulnerability to Verteporfin in EGFR-mutant Glioblastoma. *Clin Cancer Res*. 2021 Mar 1;27(5):1553–1569. doi: 10.1158/1078-0432.CCR-20-0018.
 21. Vogelbaum MA, Krivosheya D, Borghei-Razavi H, Sanai N, Weller M, Wick W, Soffietti R, Reardon DA, Aghi MK, Galanis E, Wen PY, van den Bent M, Chang S. Phase 0 and window of opportunity clinical trial design in neuro-oncology: a RANO review. *Neuro Oncol*. 2020 Nov 26;22(11):1568–1579. doi: 10.1093/neuonc/noaa149.
 22. Sanai N. Phase 0 Clinical Trial Strategies for the Neurosurgical Oncologist. *Neurosurgery*. 2019 Dec 1;85(6):E967-E974. doi: 10.1093/neuros/nyz218.
 23. Jonas O, Landry HM, Fuller JE, Santini JT Jr, Baselga J, Tepper RI, Cima MJ, Langer R. An implantable microdevice to perform high-throughput in vivo drug sensitivity testing in tumors. *Sci Transl Med*. 2015 Apr 22;7(284):284ra57. doi: 10.1126/scitranslmed.3010564.
 24. Bhagavatula S, Thompson D, Ahn SW, Upadhyaya K, Lammers A, Deans K, Dominas C, Ferland B, Valvo V, Liu G, Jonas O. A Miniaturized Platform for Multiplexed Drug Response Imaging in Live Tumors. *Cancers (Basel)*. 2021 Feb 6;13(4):653. doi: 10.3390/cancers13040653.
 25. Dominas C, Bhagavatula S, Stover E, Deans K, Larocca C, Colson Y, Peruzzi P, Kibel A, Hata N, Tsai L, Hung Y, Packard R, Jonas O. The Translational and Regulatory Development of an Implantable Microdevice for Multiple Drug Sensitivity Measurements in Cancer Patients. *IEEE Trans Biomed Eng*. 2022 Jan;69(1):412–421. doi: 10.1109/TBME.2021.3096126.
 26. Dominas C, Deans K, Packard R, Jonas O. Preparation and sterilization of an implantable drug-delivery microdevice for clinical use. *MethodsX*. 2021 May 13;8:101382. doi: 10.1016/j.mex.2021.101382.
 27. Davidson SM, Jonas O, Keibler MA, Hou HW, Luengo A, Mayers JR, Wyckoff J, Del Rosario AM, Whitman M, Chin CR, Condon KJ, Lammers A, Kellersberger KA, Stall BK, Stephanopoulos G, Bar-Sagi D, Han J, Rabinowitz JD, Cima MJ, Langer R, Vander Heiden MG. Direct evidence for cancer-cell-autonomous extracellular protein catabolism in pancreatic tumors. *Nat Med*. 2017 Feb;23(2):235–241. doi: 10.1038/nm.4256.
 28. Ahn SW, Ferland B, Jonas OH. An Interactive Pipeline for Quantitative Histopathological Analysis of Spatially Defined Drug Effects in Tumors. *J Pathol Inform*. 2021 Sep 16;12:34. doi: 10.4103/jpi.jpi_17_21.
 29. Sanai N, Polley MY, McDermott MW, Parsa AT, Berger MS. An extent of resection threshold for newly diagnosed glioblastomas. *J Neurosurg*. 2011 Jul;115(1):3–8. doi: 10.3171/2011.2.jns10998
 30. Stupp R, Gander M, Leyvraz S, Newlands E. Current and future developments in the use of temozolomide for the treatment of brain tumours. *Lancet Oncol*. 2001 Sep;2(9):552–60. doi: 10.1016/S1470-2045(01)00489-2

31. Dietlein F, Thelen L, Reinhardt HC. Cancer-specific defects in DNA repair pathways as targets for personalized therapeutic approaches. *Trends Genet.* 2014 Aug;30(8):326–39. doi: 10.1016/j.tig.2014.06.003.
32. Nguyen QD, Lavdas I, Gubbins J, Smith G, Fortt R, Carroll LS, Graham MA, Aboagye EO. Temporal and spatial evolution of therapy-induced tumor apoptosis detected by caspase-3-selective molecular imaging. *Clin Cancer Res.* 2013 Jul 15;19(14):3914–24. doi: 10.1158/1078-0432.CCR-12-3814
33. Molinaro AM, Hervey-Jumper S, Morshed RA, Young J, Han SJ, Chunduru P, Zhang Y, Phillips JJ, Shai A, Lafontaine M, Crane J, Chandra A, Flanigan P, Jahangiri A, Cioffi G, Ostrom Q, Anderson JE, Badve C, Barnholtz-Sloan J, Sloan AE, Erickson BJ, Decker PA, Kosel ML, LaChance D, Eckel-Passow J, Jenkins R, Villanueva-Meyer J, Rice T, Wrensch M, Wiencke JK, Oberheim Bush NA, Taylor J, Butowski N, Prados M, Clarke J, Chang S, Chang E, Aghi M, Theodosopoulos P, McDermott M, Berger MS. Association of Maximal Extent of Resection of Contrast-Enhanced and Non-Contrast-Enhanced Tumor With Survival Within Molecular Subgroups of Patients With Newly Diagnosed Glioblastoma. *JAMA Oncol.* 2020 Apr 1;6(4):495–503. doi: 10.1001/jamaoncol.2019.6143.
34. Yamashita S, Yokogami K, Matsumoto F, Saito K, Mizuguchi A, Ohta H, Takeshima H. MGMT promoter methylation in patients with glioblastoma: is methylation-sensitive high-resolution melting superior to methylation-sensitive polymerase chain reaction assay? *J Neurosurg.* 2018 May 4;130(3):780–788. doi: 10.3171/2017.11.JNS171710.
35. Gallego O. Nonsurgical treatment of recurrent glioblastoma. *Curr Oncol.* 2015 Aug;22(4):e273-81. doi: 10.3747/co.22.2436.
36. Tatarova Z, Blumberg DC, Korkola Jem Heiser LM, Muschler JL, Schedin PJ, Ahn SW, Mills GB, Coussens LM, Jonas O, Gray JW. Multiple spatial systems analysis of local nanodoses drug responses predicts effective treatment combinations of immunotherapies and targeted agents in mammary carcinoma. Accepted for publication in *Nat Biomed Eng*
37. Gilad Y, Gellerman G, Lonard DM, O'Malley BW. Drug Combination in Cancer Treatment-From Cocktails to Conjugated Combinations. *Cancers (Basel).* 2021 Feb 7;13(4):669. doi: 10.3390/cancers13040669.
38. in X, Kim LJY, Wu Q, Wallace LC, Prager BC, Sanvoranart T, Gimple RC, Wang X, Mack SC, Miller TE, Huang P, Valentim CL, Zhou QG, Barnholtz-Sloan JS, Bao S, Sloan AE, Rich JN. Targeting glioma stem cells through combined BMI1 and EZH2 inhibition. *Nat Med.* 2017 Nov;23(11):1352–1361. doi: 10.1038/nm.4415.
39. Narayan RS, Molenaar P, Teng J, Cornelissen FMG, Roelofs I, Menezes R, Dik R, Lagerweij T, Broersma Y, Petersen N, Marin Soto JA, Brands E, van Kuiken P, Lecca MC, Lenos KJ, In 't Veld SGJG, van Wieringen W, Lang FF, Sulman E, Verhaak R, Baumert BG, Stalpers LJA, Vermeulen L, Watts C, Bailey D, Slotman BJ, Versteeg R, Noske D, Sminia P, Tannous BA, Wurdinger T, Koster J, Westerman BA. A cancer drug atlas enables synergistic targeting of independent drug vulnerabilities. *Nat Commun.* 2020 Jun 10;11(1):2935. doi: 10.1038/s41467-020-16735-2.

40. Grossman SA, Ye X, Lesser G, Sloan A, Carraway H, Desideri S, Piantadosi S; NABTT CNS Consortium. Immunosuppression in patients with high-grade gliomas treated with radiation and temozolomide. *Clin Cancer Res.* 2011 Aug 15;17(16):5473–80. doi: 10.1158/1078-0432.CCR-11-0774.
41. Litterman AJ, Zellmer DM, Grinnen KL, Hunt MA, Dudek AZ, Salazar AM, Ohlfest JR. Profound impairment of adaptive immune responses by alkylating chemotherapy. *J Immunol.* 2013 Jun 15;190(12):6259–68. doi: 10.4049/jimmunol.1203539.
42. Karachi A, Dastmalchi F, Mitchell DA, Rahman M. Temozolomide for immunomodulation in the treatment of glioblastoma. *Neuro Oncol.* 2018 Nov 12;20(12):1566–1572. doi: 10.1093/neuonc/noy072.
43. Jordan JT, Sun W, Hussain SF, DeAngulo G, Prabhu SS, Heimberger AB. Preferential migration of regulatory T cells mediated by glioma-secreted chemokines can be blocked with chemotherapy. *Cancer Immunol Immunother.* 2008 Jan;57(1):123–31. doi: 10.1007/s00262-007-0336-x.
44. Jonas O, Calligaris D, Methuku KR, Poe MM, Francois JP, Tringhese F, Changelian A, Sieghart W, Ernst M, Krummel DA, Cook JM, Pomeroy SL, Cima M, Agar NY, Langer R, Sengupta S. First In Vivo Testing of Compounds Targeting Group 3 Medulloblastomas Using an Implantable Microdevice as a New Paradigm for Drug Development. *J Biomed Nanotechnol.* 2016 Jun;12(6):1297–302. doi: 10.1166/jbn.2016.2262.

Table 1

Table 1 is available in the Supplementary Files section.

Figures

Figure 1

Intratumoral Microdevices. **a:** Photography of microdevice in real dimensions, compared to a pencil tip. Each number represent the independent outlet of each reservoir. **b:** List of drugs contained in the IMD. **c:** Cartoon representing the rationale for using IMD. **d:** Trial schema

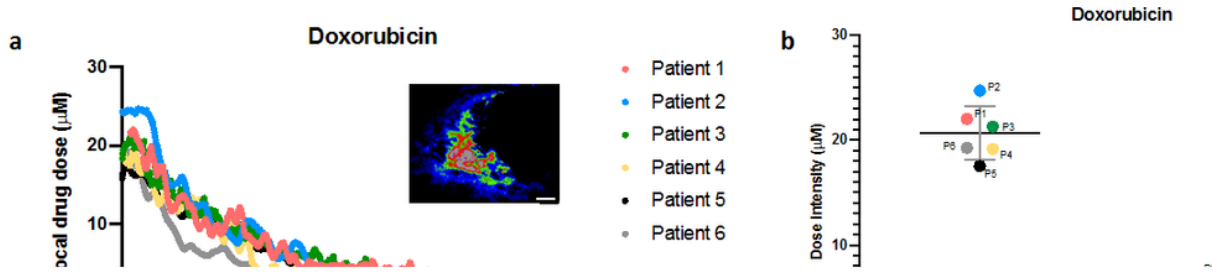


Figure 2

Drug release profiles from each patient for Doxorubicin (**a**) and Lapatinib (**c**). Inset shows typical 2-dimensional spatial profile of drug distribution. Inset scale bar is 200mm. The variation in maximum and average dose for each drug between patients is shown in (**b,d**). Error bars represent standard deviation.

Figure 3

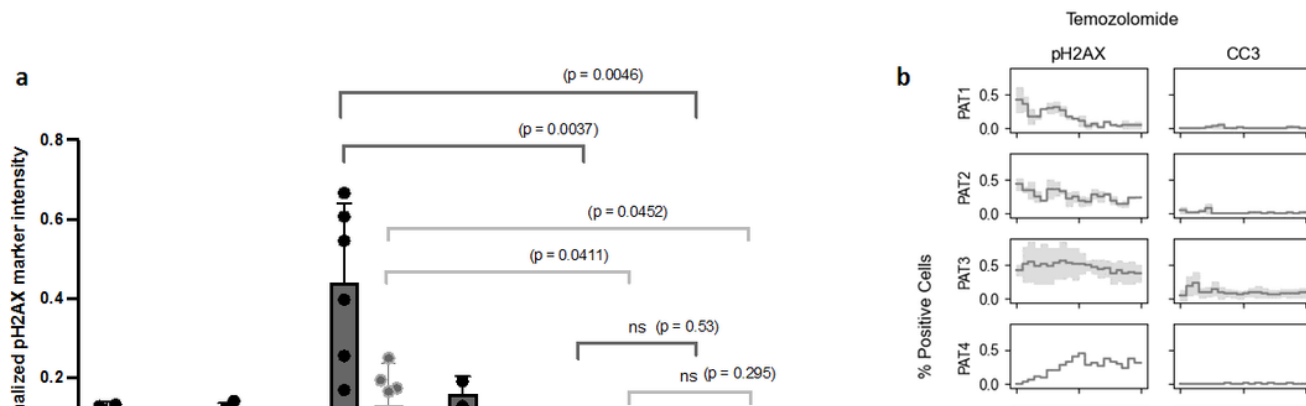


Figure 3

Differential tumor response to temozolomide. a: Quantification of IHC stains for pH2AX and CC3 in IMD tissue from each numbered patient. Each point represents a measurement from a distinct tumor region comprising 800mm x 400mm exposed to drug. Bars display mean and standard deviation. Pairwise comparisons use unpaired t-test, with two-tailed p-values shown in parentheses. **b:** Distance and concentration dependent analysis of pH2AX and CC3 stains across the six patients. Graphs are shown as mean (black) and standard deviation (grey) where available.

Figure 4

Clinical-molecular correlates. a: time-course MRIs of three representative patients who received systemic therapy after surgery and IMD analysis. **b:** Quantification of specific in-situ response to TMZ (by pH2AX immunostaining) for each patient in the study as determined by IMD analysis. Each point represents a measurement from a distinct tumor region comprising 800mm x 400mm exposed to drug. Bars display mean and standard deviation. Pairwise comparisons use unpaired t-test, with two-tailed p-values shown in parentheses **c:** Survival data for each patient in the study, including type and timing of adjuvant therapy administered.

Specific patients are color-coded to show correlation among radiologic data, IMD response and tumor response.

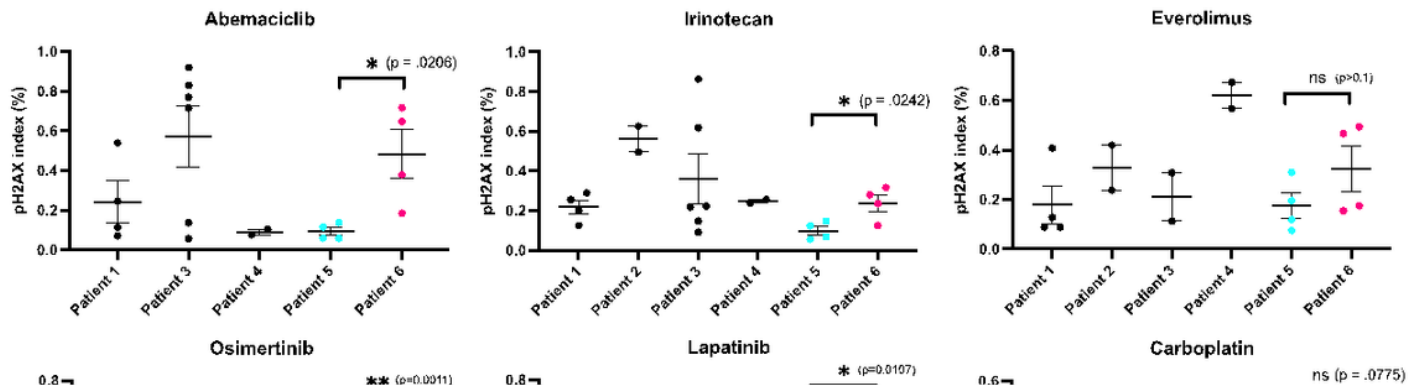


Figure 5

Personalized tumor responses to different drugs. Comparison of tumor response to several agents by DNA damage (pH2AX). Values are expressed as a normalized marker index for all cells in drug-exposed tumor regions. Mean and standard error are shown. Patient 5 (cyan) and Patient 6 (magenta) are highlighted, and pairwise comparisons are made between them using unpaired t-tests with two-tailed p-values.

Supplementary Files

This is a list of supplementary files associated with this preprint. Click to download.

- [Onlinefloatimage4.png](#)
- [Onlinefloatimage11.png](#)
- [Onlinefloatimage2.png](#)
- [Onlinefloatimage5.png](#)
- [Onlinefloatimage8.png](#)
- [Onlinefloatimage3.png](#)